Mechanosensitive EPLIN-dependent remodeling of adherens junctions regulates epithelial reshaping

Katsutoshi Taguchi, Takashi Ishiuchi, and Masatoshi Takeichi

RIKEN Center for Developmental Biology, Minatojima-Minamimachi, Chuo-ku, Kobe 650-0047, Japan

The zonula adherens (ZA), a type of adherens junction (AJ), plays a major role in epithelial cell–cell adhesions. It remains unknown how the ZA is remodeled during epithelial reorganization. Here we found that the ZA was converted to another type of AJ with punctate morphology (pAJ) at the margins of epithelial colonies. The F-actin–stabilizing protein EPLIN (epithelial protein lost in neoplasm), which functions to maintain the ZA via its association with αE-catenin, was lost in the pAJs. Consistently, a fusion of αE-catenin and EPLIN contributed to the formation of ZA but not pAJs. We show that junctional tension was important for retaining EPLIN at AJs, and another force derived from actin fibers laterally attached to the pAJs inhibited EPLIN–AJ association. Vinculin was required for general AJ formation, and it cooperated with EPLIN to maintain the ZA. These findings suggest that epithelial cells remodel their junctional architecture by responding to mechanical forces, and the αE-catenin–bound EPLIN acts as a mechanosensitive regulator for this process.

Introduction

Many classes of epithelial cells adhere to each other via zonula adherens (ZA), an epithelial form of the adherens junction (AJ). The ZA consists of E-cadherin–catenin complexes and associated actin filaments, called circumferential actin cables, and is located at a region near the apical end of lateral cell–cell contacts, showing a closed ring configuration (Farquhar and Palade, 1963; Boller et al., 1985; Cavey and Lecuit, 2009; Meng and Takeichi, 2009). αE-catenin, which binds to E-cadherin via β-catenin, mediates the interactions between the E-cadherin–β-catenin complex and actin filaments (Kovacs and Yap, 2008; Nelson, 2008; Meng and Takeichi, 2009; Sawyer et al., 2009; Kwiatkowski et al., 2010). Although the E-cadherin–β-catenin–αE-catenin complex cannot directly bind to actin filaments (Drees et al., 2005; Yamada et al., 2005), other actin-binding proteins attached to αE-catenin appear to assist in their linkage. These proteins include EPLIN (epithelial protein lost in neoplasm; Abe and Takeichi, 2008) and vinculin (Geiger et al., 1980; Watabe-Uchida et al., 1998; le Duc et al., 2010; Yonemura et al., 2010), which bind the VH3 domain and a portion between the VH1 and VH2 domains of αE-catenin, respectively. EPLIN has the ability to stabilize actin filaments (Maul et al., 2003), and in turn maintains the circumferential actin cables (Abe and Takeichi, 2008). Vinculin anchors actin filaments to the integrin-mediated focal contacts (Ziegler et al., 2006; Parsons et al., 2010) and is localized along the AJs, although its role in AJ formation is not well understood. The presence of such mediators between the cadherin and F-actin systems suggests that their interactions are regulatable. Cells may use this potentially dynamic linkage of the two systems to transmit mechanical forces generated by the cytoskeleton to cell junctions and vice versa, so as to regulate cell shape and other properties of the cells.

During development or pathogenetic processes, epithelial sheets undergo dynamic cell rearrangement, such as epithelial–mesenchymal transition, convergent extension, migration, and folding (Thiery, 2002; Montell, 2008; Acloque et al., 2009; Harris et al., 2009; Kalluri and Weinberg, 2009). For these processes, the regulation of AJs is thought to be important (Perez-Moreno et al., 2003; Lecuit, 2005). One AJ-related morphogenetic process is embryonic epithelial closure or wound healing, in which epithelial sheets fuse to one another via AJs (Jacinto et al., 2000; Vasioukhin and Fuchs, 2001; Gorfinkiel and Arias, 2007; Solon et al., 2009; Laplante and Nilson, 2011). During wound closure, "purse string–like" actomyosin cables are organized along the margins of the leading edges of the cells, and these cables gradually contract to close the open space

Correspondence to Masatoshi Takeichi: takeichi@cdb.riken.jp

Abbreviations used in this paper: AJ, adherens junction; EPLIN, epithelial protein lost in neoplasm; lAJ, linear AJ; pAJ, punctate AJ; ROCK, Rho kinase; ZA, zonula adherens.

The Rockefeller University Press $30.00
J. Cell Biol. Vol. 194 No. 4 643–656
www.jcb.org/cgi/doi/10.1083/jcb.201104124

(Franke et al., 2005; Miyake et al., 2006; Tamada et al., 2007). These actomyosin cables are linked to the AJs, which suggests that the cell–cell adhesion and cytoskeletal functions coordinate to achieve the proper reorganization of epithelial sheets.

In the present study, we investigated the mechanisms of the interplays between αE-catenin and associated actin-binding proteins, which are involved in epithelial junctional remodeling. The ZA has a closed ring structure. However, at the margin of epithelial colonies, the ZAs are autonomously converted to another form of AJ, punctate AJs. This junctional remodeling seems to be important for epithelial sheets to undergo their fusion with other sheets. We found that EPLIN functions as a mechanosensor for this process. We also found that vinculin is indispensable for general AJ formation, and it cooperates with EPLIN in maintaining the ZAs. These findings provide evidence showing that the interactions between αE-catenin and actin-binding proteins play critical roles in epithelial junctional remodeling.

Results

Two forms of AJs in epithelial colonies

Double immunostaining for E-cadherin and F-actin showed that colonies of DLD1 epithelial cells, a polarized epithelial cell line derived from human colon carcinoma, exhibit two forms of AJ. In the inner portions of the colonies, cells organized the typical, closed ZAs, where E-cadherin and F-actin are linearly aligned. At the margins of the colonies, in contrast, the junctions were opened toward cellular free edges (Fig. 1, A and B). Although these open junctions were structurally equivalent to the ZA at the interior portions, they lost the linearity near the free edges, where E-cadherin signals became discontinuous. In some of these peripheral cells, E-cadherin maintained a closed ring structure, even though these cells have no contact partners at the side of their leading edges (Fig. S1 A). From a morphological point of view, this ring is likely a remnant of the ZA. Cells with the closed and open E-cadherin signals were detectable within a single colony (Fig. S1 A), which suggests that these structures are convertible. Throughout this paper, we call the peripheral AJs punctate AJs (pAJs), and the inner AJs forming ZAs are called linear AJs (lAJs). E-cadherin and αE-catenin always colocalized at both types of AJ (Fig. S1 A).

To investigate the cytoskeletal backgrounds for these junctional structures, we looked at F-actin distributions. The peripheral cells organized actin bundles running in parallel with the cellular edge. These actin bundles terminated at the pAJs at right angles, where individual E-cadherin puncta were morphologically pulled toward the associated actin filaments (Fig. 1, A and B), as seen in mesenchymal or fibroblastic AJs (Miyake et al., 2006). This type of actin association pattern is shown in contrast with the parallel alignment of F-actin and E-cadherin at the lAJs. We also examined the distributions of myosin II isoforms IIA and IIB, which have recently been shown to work differently in AJ formation (Ivanov et al., 2007; Smutny et al., 2010). Myosin IIA was localized along the ZAs, as well as along the peripheral actin fibers targeting the pAJs (Fig. 1 C, top). Myosin IIB also densely delineated the ZAs, but it only locally decorated the peripheral actin fibers (Fig. 1 C, bottom). As found for E-cadherin or αE-catenin, myosin IIB often exhibited a closed ring configuration in the peripheral cells, which suggests that not only the authentic ZAs but also the peripheral ZA-like rings comprise actomyosin filaments and associated E-cadherin–catenin complexes.

The pAJ-associated actin (or actomyosin) fibers were reminiscent of the purse string–like actin cables formed by cells undergoing wound closure (Yonemura et al., 1995; Adams et al., 1996; Vasioukhin et al., 2000). To confirm this, we purposely scratched DLD1 cell layers. We found that the cells whose neighbors were removed remodeled their linear junctions to form the punctate type with concomitant reorganization of actin fibers (Fig. S1 B). We therefore assumed that the linear-to-nonlinear conversion of AJs taking place at the margins of stationary DLD1 colonies is identical to the process that occurs in acute wound closure. We also noticed that, when two cell colonies touched one another, a fraction of the peripheral actin fibers turned to these new contacts, exhibiting an actin–AJ configuration similar to that in pAJs (Fig. 1 D). This suggests that the pAJs are equivalent to newly formed cell–cell contacts. Similar morphological conversion of AJs at colony margins was seen in a wide variety of polarized epithelial cells, such as MDCK, EpH4, and Caco2 cells, which suggests that this process generally occurs in epithelial cells. We thus decided to study the mechanisms of this junctional remodeling and its role in epithelial closing behavior.

E-cadherin and αE-catenin dynamics at colony peripheries

To compare the pAJs and lAJs from a dynamic viewpoint, we transfected DLD1 cells with E-cadherin–monomeric Kusabira orange (mKOR), and its αE-catenin–deficient variant R2/7 cells (Watabe-Uchida et al., 1998) with αE-catenin–EGFP; we then collected live images of the fluorescent signals from these transfectants. Both probes gave essentially identical results, which supports the idea that these two molecules behave together as a complex. E-cadherin signals forming pAJs were extremely dynamic, quickly changing their shape (Video 1); these signals were often pulled in a direction parallel to the cellular edges. We also captured an image in which an open ZA ring is transiently closed with moving E-cadherin clusters (Video 1, left). Curiously, in the cells forming a stable E-cadherin ring, E-cadherin puncta forming pAJs constantly flowed into the ring structures (Video 1, right). However, the lAJs in these colonies were relatively stable.

We also performed similar imaging during epithelial wound healing. We scratched confluent DLD1 cell layers, and observed the cells that had been exposed to an open space. Time-lapse imaging of αE-catenin–EGFP showed that cells moved toward the open space with leading edges, and as soon as they touched those moving from the opposite side, αE-catenin promptly accumulated at their contact points in a pAJ-like fashion (Video 2). When these cells had a closed αE-catenin–EGFP ring, its front rim was disrupted before touching another cell. These observations confirmed that the pAJ-type junctions take part in nascent cell–cell contacts.

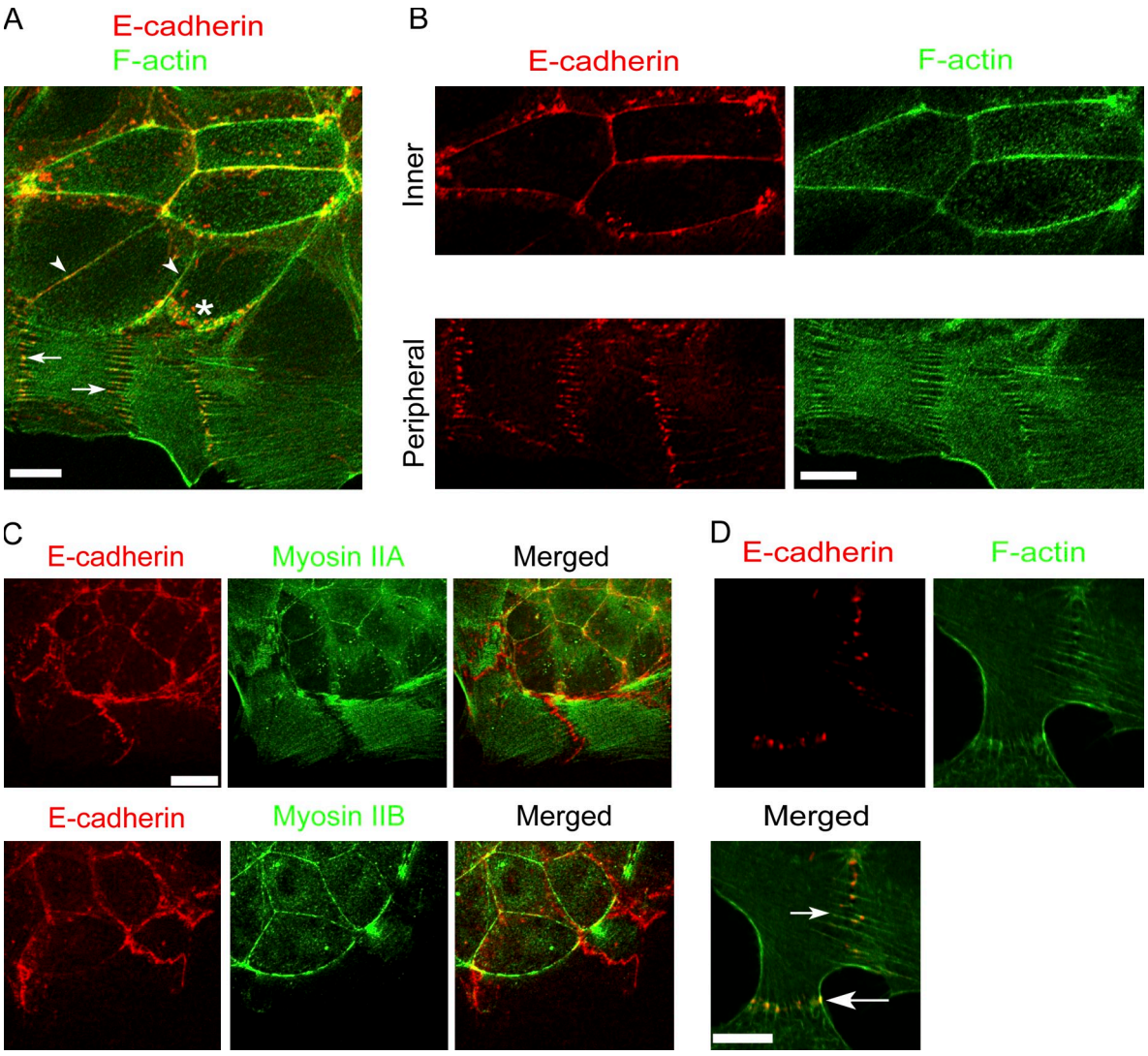

Figure 1. **Two types of AJ in a DLD1 colony.** (A) Projected confocal images of a colony of DLD1 cells double-immunostained for E-cadherin and F-actin. Arrowheads and arrows point to linear and punctate portions of the AJ outlining a peripheral cell, respectively. Asterisk, a putative ZA remnant. (B) The same image as in A, but focused on apical and basal planes of the colony, highlighting ZAs in inner cells and pAJs in peripheral cells, respectively. At the ZAs, linear E-cadherin and F-actin signals closely colocalize with each other, whereas E-cadherin signals at pAJs are associated with the terminals of peripheral actin fibers. (C) Projected confocal images of myosin IIA or IIB, immunostained together for E-cadherin. Both isoforms delineate ZAs. In addition, myosin IIA decorates peripheral F-actins, and IIB organizes a closed ring even in peripheral cells. (D) The small arrow points to a pAJ of a colony, and the large arrow indicates a contact point between this colony and another colony. Note that these two junctions were morphologically similar to one another. Bars, 10 µm.

Live imaging of actin-EGFP introduced into DLD1 cells showed that the peripheral actin fibers were highly dynamic, as observed for pAJ-forming E-cadherin, whereas ZA-associated F-actin was much more stable (Video 3). Arrays of actin clusters, which are assumed to correspond to those associated with pAJs, were pulled in directions parallel to the cellular edges, which suggests that strong tension is operating on them. Some of these actin clusters moved inward, which suggests that the observed E-cadherin flow might have been driven by these actins via their linkages.

EPLIN localizes only at lAJs and is responsible for their formation

To study the mechanisms of the junctional conversion, we investigated the molecular differences between these two forms of AJs. Major E-cadherin–associated proteins and β-, α-, and p120-catenins were localized in both forms of the junction in proportion to E-cadherin. Likewise, vinculin, ZO-1, and afadin, which are known to interact with αE-catenin directly or indirectly, were detected both along the lAJs and at the pAJs (Fig. 2 A, left; and Fig. S2, A and B). Intriguingly, another αE-catenin–interacting protein, EPLIN, was detected only at the lAJs, not at the pAJs, although EPLIN decorated peripheral actin fibers in immediate proximity to E-cadherin puncta forming the pAJs (Fig. 2 A, right). We also noticed that some of the epithelial lines, including MCF10A cells, exhibit pAJ-type junctions throughout their colonies, and these junctions were devoid of EPLIN signals (Fig. S2 C). Thus, EPLIN seems to be localized to only lAJs across cell lines.

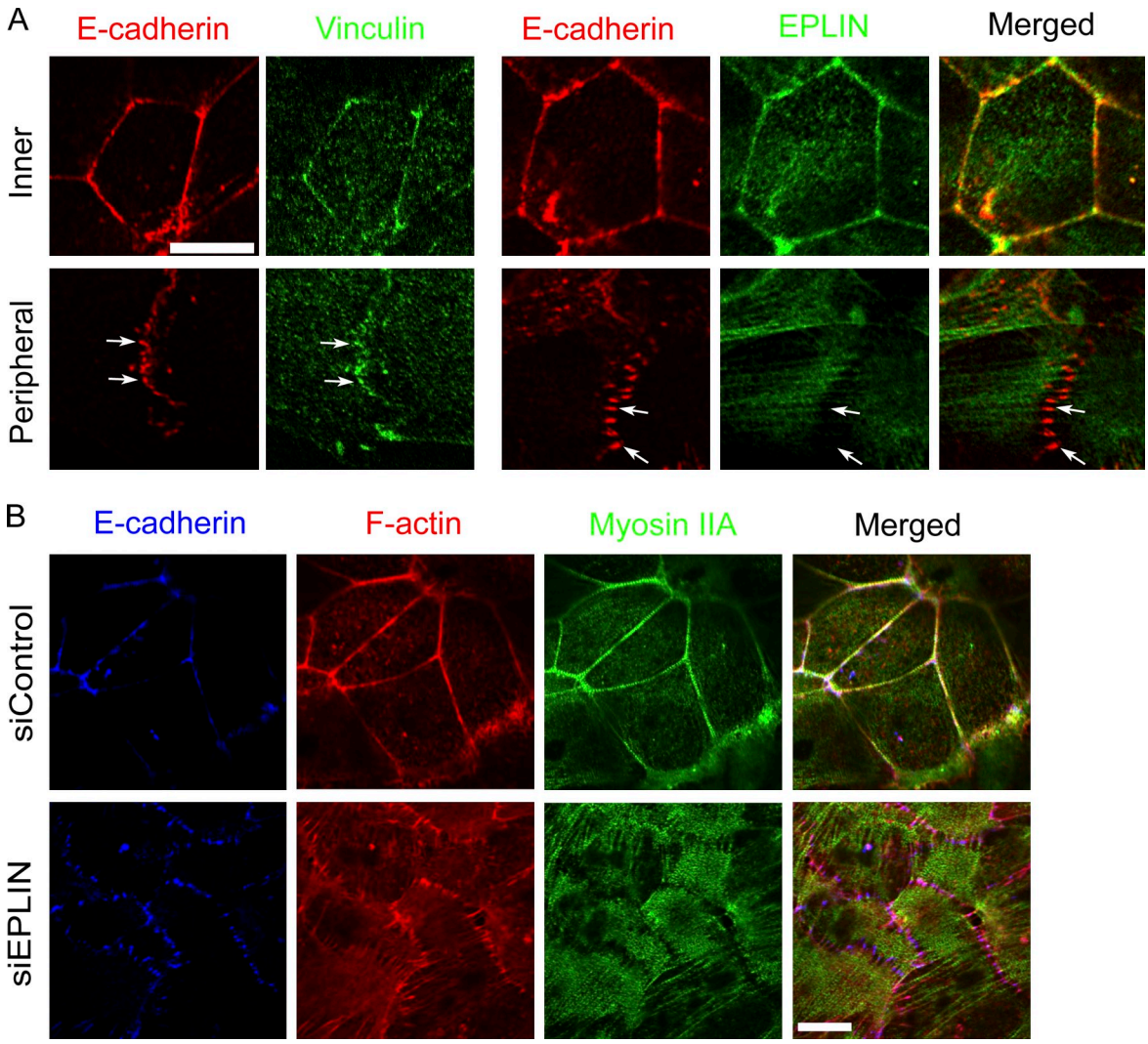

Figure 2. **EPLIN is specifically important for ZA formation.** (A) Double-immunostaining for E-cadherin and vinculin (left) or EPLIN (right). Images are focused on ZAs in inner cells and pAJs in peripheral cells. Vinculin colocalizes with E-cadherin in both lAJs and pAJs, whereas EPLIN is not detectable in pAJs. Arrows point to typical E-cadherin signals, associated with vinculin or not associated with EPLIN. (B) The effects of EPLIN depletion on junctional organization. Cells located in the inner portion of the colony were double-immunostained for F-actin and myosin IIA. Note that the junction morphology in EPLIN-depleted (siEPLIN) cells is similar to that observed in the peripheral cells of control colonies (see Fig. 1 C). Bars, 10 µm.

We previously reported that EPLIN depletion caused disorganization of the ZA (Abe and Takeichi, 2008). We confirmed this in the present study by immunostaining EPLIN-depleted cells for myosin IIA. The resultant junctions were similar to pAJs (Fig. 2 B); that is, both junctions were associated with myosin IIA fibers at right angles. Time-lapse recording of E-cadherin–EGFP showed that the junctions of EPLIN-depleted cells were highly dynamic, constantly changing their shapes (Video 4), just as seen in pAJs in control cells. These observations suggest that the pAJs were generated via a mechanism that also removes EPLIN from AJs.

EPLIN localization at AJs is mechanosensitive

We then asked how EPLIN was lost from pAJs. We found that, even when EPLIN was overexpressed, this protein was never recruited to the pAJs (Fig. S3 A), which indicates that there must be an active mechanism to suppress its association with the peripheral junctions. Because the pAJs are unique in their association with peripheral actin fibers, we attempted to mechanically ablate these fibers. We prepared DLD1 cells transfected with EPLIN-EGFP and E-cadherin–mKOR, in which the exogenous EPLIN-EGFP widely decorated actin fibers. Then, we laser-irradiated a peripheral cell, focusing on a tiny point on the pAJ-targeting actin fibers (Fig. 3 A). The treated actin fibers immediately retracted toward the cell–cell boundary, where they anchored (Fig. 3 B and Video 5). Simultaneously, the cell connected with the laser-treated cell via the pAJ also contracted, likely because of the loss of a tension balance between the two cells. At the cell–cell boundary between these laser-treated and untreated cells, EPLIN signals were quickly up-regulated in a form of lAJ at the original pAJ sites, which suggests that removal of the peripheral actin fiber–derived force is sufficient to restore lAJs at these sites. This up-regulation of EPLIN accompanied a simultaneous increase of E-cadherin at the same cell boundaries (Fig. S4 [A and B] and Video 6), which indicates that EPLIN and E-cadherin behave together during these changes.

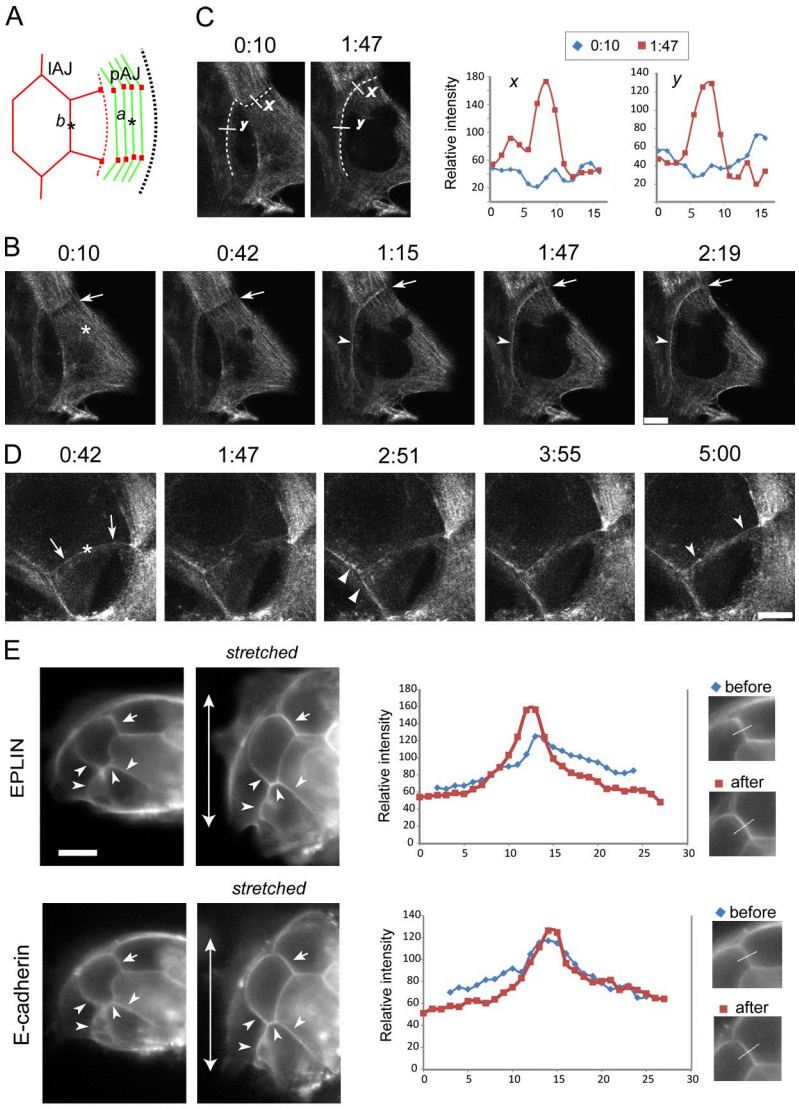

Figure 3. **Mechanosensitive nature of EPLIN and E-cadherin localization.** (A) Schematic drawing of the points for laser irradiation. Peripheral actin bundles (a) or a part of the ZA (b) were cut with a laser. (B) Time-lapse images of EPLIN-EGFP after the laser irradiation at "a" (asterisk). Arrows indicate the original position of pAJ, which was inferred by the reduced EPLIN signals. EPLIN immediately accumulated at this position, with a concomitant up-regulation of EPLIN along the entire contiguous junctions (arrowhead). See also Video 5. A typical example of multiple experiments is shown. (C) Choosing two time points in B, cell–cell boundaries are traced with dotted lines. Relative fluorescence intensity across the cell boundaries was also measured at the sites marked as "x" and "y." (D) Time-lapse images of EPLIN-EGFP after laser irradiation at "b." Arrows in the first panel point to the original linear EPLIN signals: these signals were temporarily disordered or faded out, but reappeared at 5:00, as indicated by arrowheads in the last panel. Arrowheads in middle panels point to a transient up-regulation of EPLIN fluorescence signals, in which fluorescence increased ∼30% at 2:51. See also Video 7. (E) DLD1 cells double-transfected with E-cadherin–mKOR and EPLIN-EGFP were stretched to ∼150% of their original length. A typical colony is shown. Line profiles of fluorescence of E-cadherin–mKOR or EPLIN-EGFP signals across the junction, indicated by arrows, are shown at the right. Other junctions exhibiting similar changes are indicated with arrowheads. Quantification of fluorescence showed that the peak intensity of E-cadherin–mKOR and EPLIN-EGFP signals increased 18% (18 ± 08, $n = 15$, $P < 0.05$) and 17% (17 ± 07, $n = 15$, $P < 0.05$), respectively, in the junctions of stretched cells. Data represent mean ± SEM. Three independent experiments were performed. before, before stretch; after, after stretch. Time points are given in minutes and seconds. Bars, 10 µm.

Importantly, the above laser ablation also induced the straightening of the entire junction continuous to the affected pAJs (Fig. 3 C). Furthermore, up-regulation of EPLIN occurred not only at the original pAJ sites but also throughout these straightened junctions (Fig. 3 B). These observations suggested that some mechanical changes were induced in these junctions as a result of the cytoplasmic actin ablation, and these changes might have promoted the recruitment of EPLIN and E-cadherin to them. To test this idea further, we asked what would happen at the junctions where their internal tension is removed. We lightly irradiated part of the ZA, focusing on a middle point between the vertexes, avoiding their complete disruption. In the severed junctions, EPLIN signals became irregular, and some diffused away 3–4 min after laser treatment (Fig. 3 D and Video 7), although the linear EPLIN signals began to recover around 5 min in the example specimen shown here. We also monitored E-cadherin–mKOR after similar laser cutting of ZAs, and found that E-cadherin signals gradually faded during the 5-min observations (Fig. S4 C). These results suggest that mechanical forces such as tension support the proper accumulation of EPLIN and E-cadherin at lAJs. In these experiments, we also noticed that EPLIN signals fluctuate in nontreated junctions contiguous to the laser-treated junction via a vertex (Fig. 3 D, arrowheads in the center panel; and Video 7), where we suppose that the tension acting on the former was altered because of the laser ablation of the latter.

To confirm the role of tension, we used a stretching machine to test whether external forces can also affect the EPLIN and E-cadherin association with lAJs (Iwaki et al., 2009). We cultured DLD1 colonies consisting of several cells on an elastic chamber, and stretched them unidirectionally to ∼150% of their original length. In the treated colonies, the cell–cell boundaries lengthened or shortened to varying degrees, depending on their directions. Live images of transfected EPLIN-EGFP and E-cadherin–mKOR showed that their signals were sharpened or intensified at the majority of the junctions (Fig. 3 E; see the figure legend for quantification). These observations suggest that the accumulation of EPLIN and E-cadherin

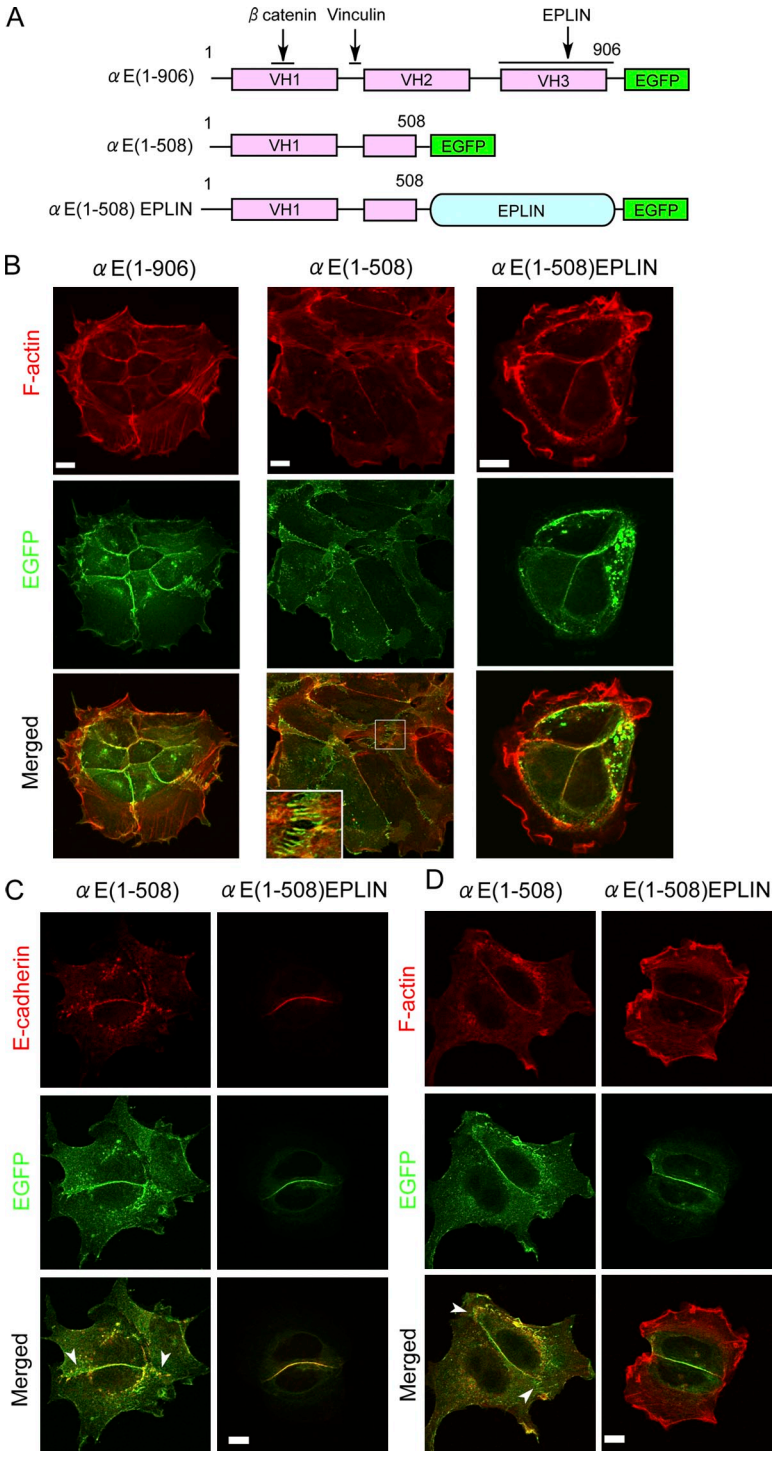

Figure 4. **Exogenous expression of an αE-catenin–EPLIN fusion in R2/7 cells.** (A) αE-catenin constructs tagged with EGFP. αE(1–906) corresponds to the full-length αE-catenin. The full-length EPLIN was fused to αE(1–508). (B) Junctional organization in R2/7 cells transfected with αE(1–906), αE(1–508), or αE(1–508)EPLIN. Contrasted with the balanced organization of lAJs and pAJs in αE(1–906)-transfected colonies, αE(1–508) transfectants show pAJs even in the interior. The inset shows an enlarged view of the boxed region. αE(1–508)EPLIN organize only lAJ-like junctions. Dotted signals probably represent overexpressed molecules deposited in the cytoplasm. (C and D) Junctional organization in R2/7 cells transfected with αE(1–508) or αE(1–508)EPLIN. Cells were double-stained for EGFP and E-cadherin (C) or F-actin (D). αE(1–508) organizes lAJs and pAJs at the central and peripheral regions, respectively, whereas αE(1–508)EPLIN organizes only lAJs. Arrowheads indicate pAJs. Bars, 10 µm.

in lAJs is affected by pull forces, which is consistent with the results observed in laser ablation experiments.

Rho kinases (ROCKs) play a major role in the contraction of actomyosin filaments localized in ZAs (Hildebrand, 2005; Nishimura and Takeichi, 2008), and this contractility is likely a major cause of junctional tension. We found that ROCK1 is localized along the lAJs but not at pAJs (Fig. S3 B). When DLD1 cells were treated with a ROCK inhibitor, Y-27632, the junctional morphology was converted to the pAJ type, and EPLIN was completely abolished from these AJs (Fig. S3 C), although vinculin still localized at these Y-27632–treated junctions (Fig. S3 D). Similar results were obtained when myosin IIA or IIB was knocked down (Fig. S5 A): as previously described (Ivanov et al., 2004; Smutny et al., 2010), myosin IIA depletion caused disorganization of E-cadherin and F-actin distributions, and EPLIN no longer colocalized with E-cadherin in these cells (Fig. S5 B). In myosin IIB–depleted cells, their junctional morphology became similar to that of pAJs, and EPLIN disappeared from these junctions.

These observations suggest that the ROCK-mediated contraction of AJ-associated actomyosin is required for the localization of EPLIN to AJs. Because EPLIN is recruited to AJs via its association with αE-catenin (Abe and Takeichi, 2008), we examined whether the αE-catenin–EPLIN interaction is maintained or not in Y-27632–treated cells by immunoprecipitation experiments. We first noticed that the detergent solubility of EPLIN was increased after Y-27632 treatments (Fig. S3 E, left), which suggests that the binding of EPLIN to actin fibers is ROCK dependent at least in part. Then, we found that a similar amount of EPLIN coprecipitated with αE-catenin in the control and Y-27632–treated cells, which indicates that their interaction was not affected by ROCK inhibition. These results indicated that the pAJs exclude the entire αE-catenin–EPLIN complex from themselves.

Altogether, these findings suggest that the lAJs maintain the αE-catenin–EPLIN complex (presumably the E-cadherin–αE-catenin–EPLIN complex) in a tension-sensitive way, and this process is blocked by peripheral actin fibers attached to the AJs from the lateral sides. At the pAJs, only the EPLIN-free E-cadherin–αE-catenin complexes are allowed to function.

αE-catenin–EPLIN fusion proteins exclusively contribute to lAJ formation

To further study the specific roles of the αE-catenin–EPLIN complex, we constructed a fusion protein between αE-catenin and EPLIN using the αE(1–508) fragment of αE-catenin, in which the EPLIN-binding VH3 domain and adjacent portions were removed (Fig. 4 A). To characterize this fusion protein (αE(1–508)EPLIN), we prepared R2/7 cells transfected with this construct (αE(1–508)EPLIN-R2/7 cells), and also those transfected with αE(1–508) as a control (αE(1–508)-R2/7 cells). R2/7 transfectants with the full-length αE-catenin (αE(1–906)-R2/7 cells) were also used for comparison. We confirmed that both αE(1–508) and αE(1–508)EPLIN coprecipitate with E-cadherin upon immunoprecipitation (Fig. 5 A).

As described previously (Watabe-Uchida et al., 1998), αE(1–508) can organize AJ-like junctions. However, αE(1–508)-R2/7 cells were different from the αE(1–906)-R2/7 cells or DLD1 cells, in that they form nonlinear junctions even in the interior of the colony (Fig. 4 B, left and middle). This suggests that the deleted portions are required for a balanced lAJ-pAJ organization. However, αE(1–508)EPLIN-R2/7 cells exhibited only linear-type junctions, and curiously αE(1–508)EPLIN signals were not detectable at peripheral regions (Fig. 4 B, right). For more precise analysis of these junctional structures, we examined a single cell–cell border formed between a pair of cells. αE(1–508) or associated E-cadherin exhibited both the linear and nonlinear configurations within the border (Fig. 4, C and D), confirming that αE(1–508) can organize into both forms of AJ. In the case of αE(1–508)EPLIN-R2/7 cells, this construct sharply delineated the cell–cell borders together with E-cadherin or F-actin (Fig. 4, C and D), but it never showed any punctate-type distribution (Fig. 4, C and D). In addition, the αE(1–508)EPLIN-mediated contacts appeared unstable, as these junctions slid by each other, and even broke up during cultures (Video 8). Intriguingly, when αE(1–508) and αE(1–508)EPLIN were coexpressed in R2/7 cells, they transiently organized a typical combination of pAJs and lAJs (Video 9): in these double transfectants, αE(1–508)EPLIN showed only ZA-like distributions, whereas αE(1–508) was localized to both pAJs and lAJs. These observations suggest that αE(1–508)EPLIN contributes to the formation of lAJ-type junctions, whereas αE(1–508) participates in both forms of AJ, and the presence of both constructs promotes the organization of AJs resembling those in normal cells.

Next, we examined the effects of the expression of αE(1–508) and αE(1–508)EPLIN in DLD1 cells on their junctional organization, designating them as αE(1–508)-DLD1 and αE(1–508)EPLIN-DLD1 cells, respectively. E-cadherin–mKOR was also cotransfected in these cells. When E-cadherin was immunoprecipitated from these transfectants, we detected both endogenous and mutant αE-catenins in the precipitates (Fig. 5 A), which suggests that E-cadherin binds either form of αE-catenin in the cells. Expression of αE(1–508) did not show any particular effects on the junctional organization in these cells. αE(1–508)EPLIN-DLD1 cells organized epithelial colonies, and the fusion protein was localized along their ZA (or lAJs), colocalizing with E-cadherin. However, in these colonies, most of the peripheral cells did not form lateral contacts, assuming a flower petal–like arrangement (Fig. 5 B). In time-lapse movies of these cells, we could detect E-cadherin signals forming pAJ-type junctions between peripheral cells. Notably, these E-cadherin signals did not colocalize with αE(1–508)EPLIN, although this fusion protein was detectable adjacent to the E-cadherin signals in a diffuse fashion. These αE(1–508)EPLIN-free E-cadherin–mediated pAJs were a transient structure, as they subsequently moved into the ZA ring formation (Fig. 5, C and D; and Video 10), as observed in wild-type cells (Video 1). In contrast to the control cells, however, once the pAJs were absorbed into the rings, the cell peripheries were never replenished with new pAJs, which explains why pAJs were not observable in fixed samples. The fusion proteins that were detectable in proximity to the initial pAJs might have competed with the natural E-cadherin–αE-catenin complex, resulting in the inhibition of further pAJ formation. In addition, we noticed that even the lAJs were unstable in αE(1–508)EPLIN-DLD1 cells; these junctions were often disrupted (Video 10).

Vinculin and EPLIN in AJ formation

The above results indicate that EPLIN is involved in the formation of lAJs but not pAJs, which suggests that other molecules cooperate with αE-catenin to organize the AJs. Because αE(1–508) is active in general AJ formation, molecules that bind this αE-catenin construct are candidates. We and others previously found that αE-catenin mutants, equivalent to αE(1–508), can bind vinculin in in vitro pull-down assays (Watabe-Uchida et al., 1998; Yonemura et al., 2010), and a fusion between these αE-catenin mutants and vinculin could organize AJs (Watabe-Uchida et al., 1998), which suggests that vinculin works together with αE-catenin. However, the role of vinculin in AJ formation has not been thoroughly investigated through loss-of-function approaches. We therefore reexamined the function of vinculin in the formation of cell–cell contacts.

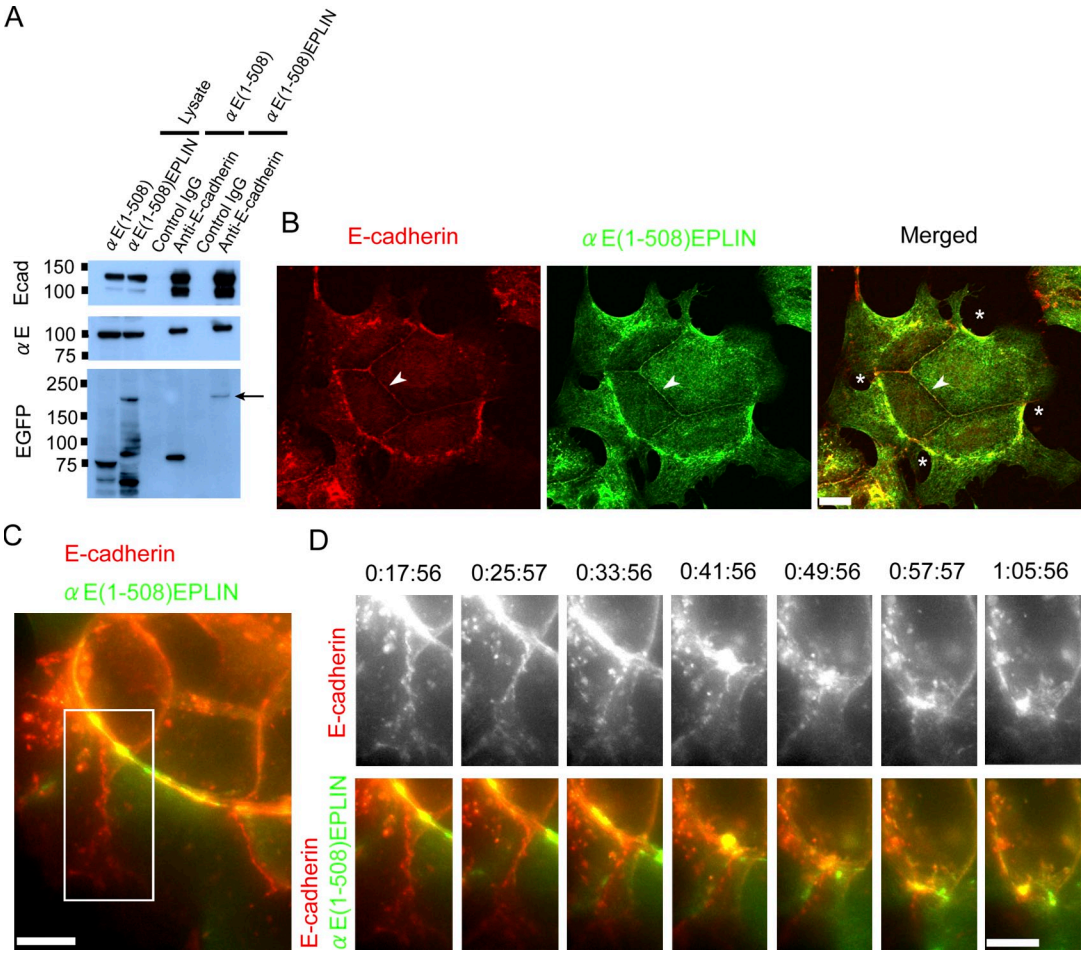

Figure 5. **Expression of αE-catenin-EPLIN fusion prohibits pAJ formation.** (A) Immunoprecipitation assays to detect coprecipitation of E-cadherin and αE(1–508) or αE(1–508)EPLIN. Lysates were collected from DLD1cells transfected with these constructs. E-cadherin immunoprecipitates contain not only endogenous αE-catenin but also these artificial proteins. Molecular masses are given in kilodaltons. Ecad, E-cadherin; αE, endogenous αE-catenin. The arrows indicate the αE(1–508)EPLIN band. (B) A representative colony of αE(1–508)EPLIN-transfected DLD1 cells. This colony does not have pAJs, as marked with asterisks. Arrowheads point to an lAJ. (C and D) Time-lapse images of E-cadherin–mKOR and αE(1–508)EPLIN-EGFP doubly transfected into DLD1 cells. A starting image is shown in C (boxed region). E-cadherin colocalizes with the fusion protein on ZA rings, but not at pAJs. pAJs were initially detected, but then gradually lost, because of their flow into the ZA ring. Time points are given in hours, minutes, and seconds. See also Video 10. Bars, 10 µm.

We first looked at the effects of vinculin depletion on the junctions of αE(1–508)-R2/7 and αE(1–508)EPLIN-R2/7 cells. In both transfectants, vinculin colocalized with these mutant molecules at cell junctions, whereas this did not occur at the contact sites between parent R2/7 cells (Fig. 6 A). This supports the idea that the vinculin-binding site is preserved in both constructs. In vinculin-specific siRNA-treated cells, vinculin levels were considerably down-regulated in an siRNA probe-specific way (Fig. 6, B and C). In these cells, vinculin remained at focal contacts, but became undetectable at many portions of the cell junctions. We found that vinculin-depleted αE(1–508)-R2/7 cells were vigorously dispersed in a vinculin level–dependent fashion, which indicates that vinculin is essential for AJ-dependent cell–cell contacts in these cells. In the case of αE(1–508)EPLIN-R2/7 cells, vinculin depletion did not particularly disrupt the junctions (Fig. 6 D), which suggests that EPLIN dominates over vinculin in maintaining the transient αE(1–508)EPLIN-mediated cell–cell contacts.

Next, we examined the effects of vinculin depletion in DLD1 cells, comparing this with EPLIN depletion. In vinculin-null junctions, E-cadherin signals became fragmented, and each fragment showed filopodia-like or dotted shapes, in contrast with the more condensed puncta representing the EPLIN-depleted junctions (Fig. 7 A). These vinculin-free E-cadherin signals colocalized only with faint amorphous actin signals, whereas EPLIN-depleted junctions were linked with tensile actin fibers (Fig. 7 B). These observations suggest that vinculin plays a role in linking the E-cadherin–catenin complex to the tensile actin fibers. Consistent with this idea, vinculin was still localized at the punctate junctions in EPLIN-depleted cells (Fig. 7 A). When vinculin and EPLIN were both depleted, filopodia-like E-cadherin signals appeared to have increased, but their phenotypes were essentially identical to those observed in vinculin-depleted cells. We noted that EPLIN was not detectable on the vinculin-free E-cadherin signals, even in vinculin-depleted cultures (Fig. 7 C). This explains why the effects of vinculin depletion and vinculin/EPLIN double depletion were not so different. The loss of EPLIN from vinculin-depleted cells might be a phenomenon equivalent to its unstable association with AJs that lost tension, which was observed in laser

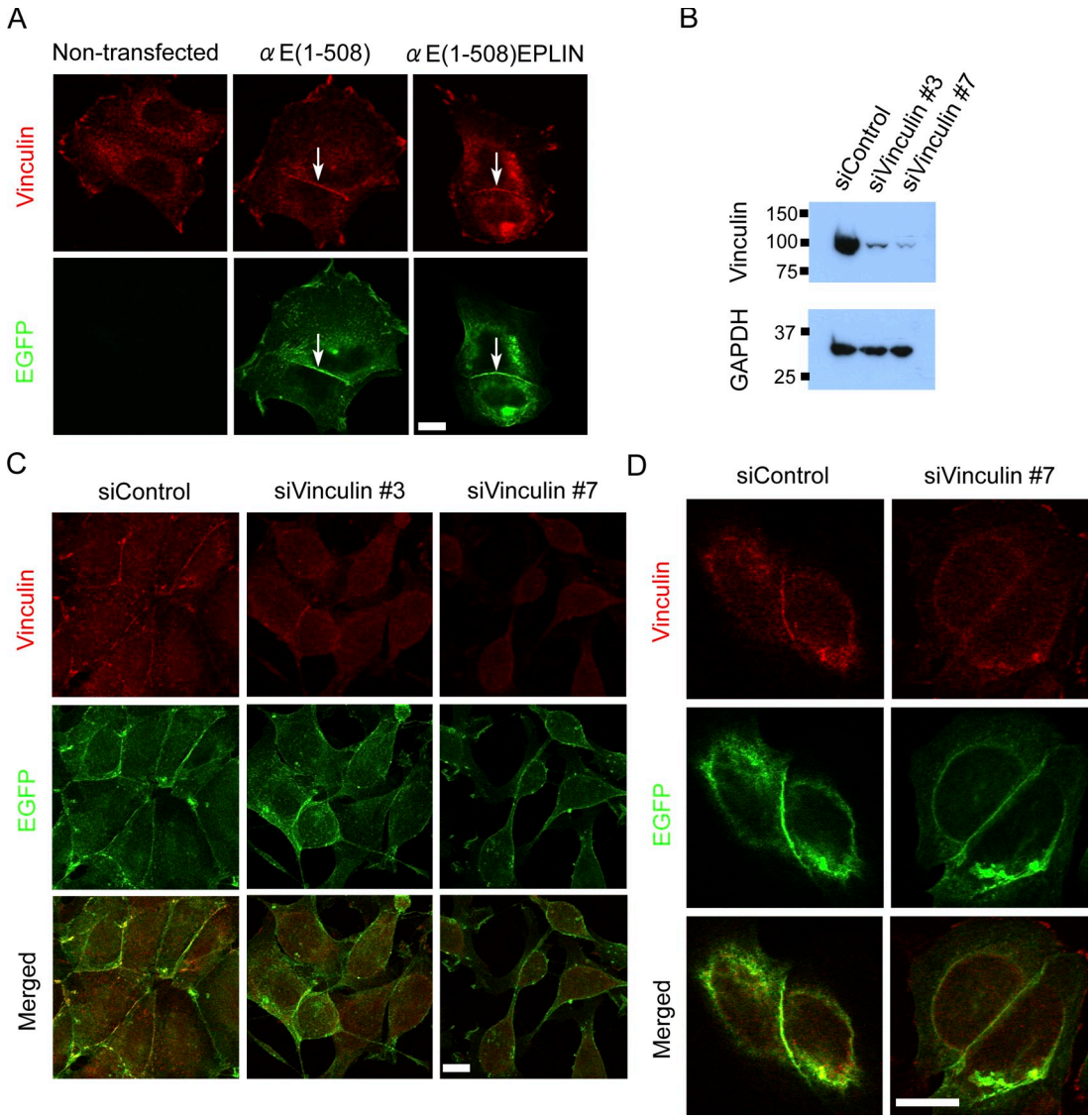

Figure 6. **The effects of vinculin depletion on R2/7 transfectants.** (A) Vinculin localization in nontransfected R2/7, αE(1–508)-R2/7, and αE(1–508)EPLIN-R2/7 cells. In both transfectants, but not in the parent cells, vinculin accumulated along cell–cell contact sites, marked with EGFP signals (arrows). (B) The vinculin level was significantly reduced by treatment with two vinculin-specific siRNA (siVinculin) probes, of which siVinculin No. 7 produced a stronger effect. Molecular mass is indicated in kilodaltons next to the gel blot. (C) Dispersion of αE(1–508)-R2/7 cells was induced by vinculin depletion. (D) The junctions of αE(1–508)EPLIN-R2/7 cells are resistant to vinculin depletion. Bars, 10 µm.

ablation experiments. Thus, EPLIN cannot maintain the stable ZAs in the absence of vinculin, although it can transiently organize lAJ-like contacts in the absence of vinculin, as shown in Fig. 6 D.

Discussion

Epithelial cells are linked together via the ZAs to form stable tissues. In embryonic or pathogenetic processes, however, epithelial sheets undergo dynamic remodeling including the closure of open spaces. We showed that the ZAs are converted to another form of AJ, pAJ, at the peripheries of cell colonies. The pAJs were involved in nascent cell–cell contacts, which suggests that the lAJ-to-pAJ conversion must be a process for epithelial cells to reorganize their junctional architecture into a more dynamic form. Our analysis of this junctional conversion demonstrated that this process is regulated through the interactions of αE-catenin with EPLIN and vinculin.

Mechanosensitive processes for the maintenance and remodeling of AJs

Previous studies suggested that the cadherin adhesion system or AJ components have mechanosensitive properties (Schwartz and DeSimone, 2008; Fernandez-Gonzalez et al., 2009; Ladoux et al., 2010; le Duc et al., 2010). Our observations indicate that at least two kinds of forces are involved in the maintenance and remodeling of epithelial AJs. One is the force derived from peripheral actin fibers targeting the pAJs. Laser ablation of the peripheral actin fibers was sufficient to convert pAJs to lAJs, which suggests that the lAJs may be a default form of AJ that

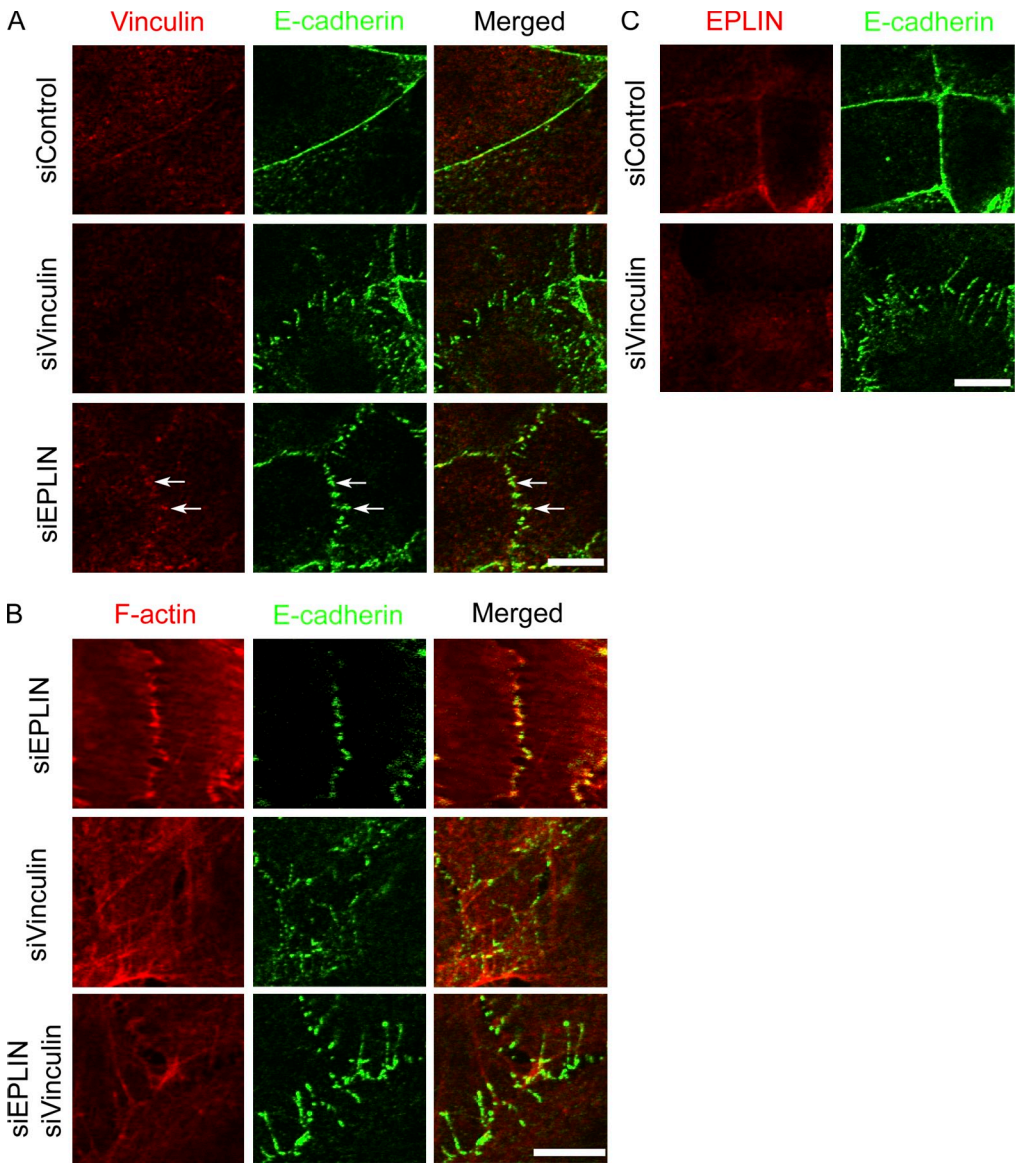

Figure 7. **The effects of vinculin depletion on DLD1 cells.** (A) Vinculin and EPLIN depletion causes fragmentation of E-cadherin signals. Vinculin remains to colocalize with E-cadherin in EPLIN-depleted cells, as indicated by arrows. (B) In vinculin-depleted and vinculin/EPLIN double-depleted cells, the fragmented E-cadherin signals no longer associate with tense actin fibers. (C) After vinculin depletion, E-cadherin no longer colocalizes with EPLIN. Bars, 10 µm.

gets reorganized by these actin fibers. The other force is the tension of lAJs, produced by ROCK-dependent contraction of themselves or by external forces. Inhibition of ROCKs or myosin II depletion abolished the lAJs, and external tension up-regulated the accumulation of EPLIN and E-cadherin on AJs. We also showed that the solubility of EPLIN increased when cells were treated with a ROCK inhibitor, which suggests that EPLIN prefers the contracting actomyosin, when it binds to actin fibers. These suggest that EPLIN maintains the lAJs sensing their tension, and that this system is impaired by the peripheral actin fibers (Fig. 8). Similar tension-dependent recruitment of AJ components was also reported for myosin II (Fernandez-Gonzalez et al., 2009).

How do the peripheral actin fibers block the association of the αE-catenin–EPLIN complex with AJs? It is noted that αE-catenin itself is a mechanosensitive protein; its conformation is altered when pulled by actin fibers, allowing its binding to vinculin (Yonemura et al., 2010). From a morphological point of view, one would expect αE-catenin to take a stretched form at pAJs, where vinculin is abundant and actin fibers are terminating in a pulling fashion. We could speculate that EPLIN is unable to bind such stretched αE-catenin molecules, and that the αE-catenin–EPLIN complex cannot interact with the pulling actin fibers; therefore, this complex is excluded from the pAJs (Fig. 8). Actually, in our previous experiments, we detected αE-catenin–EPLIN binding in vitro, where tensile forces are not expected to work on these molecular complexes (Abe and Takeichi, 2008). However, vinculin is present not only at pAJs but also at lAJs, where EPLIN localizes, which suggests that αE-catenin may also be stretched at the lAJs. This seems to contradict the model in which that EPLIN may bind only the nonstretched form of αE-catenin. However, if the ZA contains

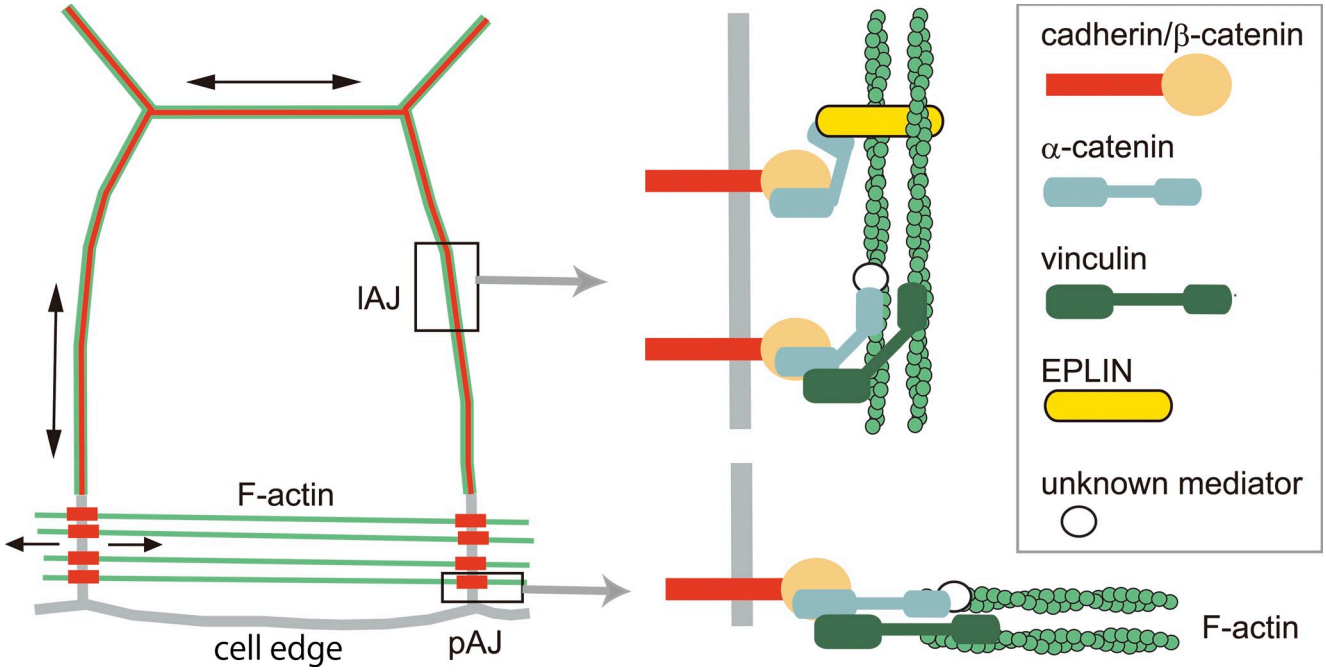

Figure 8. **Summary and model.** E-cadherin (red) and AJ-associated F-actin (green) distributions, observed in the present study, are schematically summarized at the left. At the right, a working model to explain the present observations is shown. The shapes of molecules are arbitrarily drawn. It is not determined whether EPLIN and vinculin bind to the same or different αE-catenin molecules. Black arrows indicate tension.

both the stretched and nonstretched forms of αE-catenin, the problem could be reconciled. The presence or absence of the nonstretched form of αE-catenin in the ZAs should be determined by future experiments.

How the actin fibers causing pAJ formation are generated in peripheral cells remains unknown. It is well established that actin filaments are polymerized at the cellular edges, and they show retrograde movement (Welch et al., 1997; Small and Resch, 2005). One such actin filament may play a role in the phenomena observed in the present studies. It has been shown that actomyosin cables line the leading edges of migrating cells not only during wound closure (Franke et al., 2005; Miyake et al., 2006; Tamada et al., 2007) but also at epithelial closures in normal development (Jacinto et al., 2000; Franke et al., 2005; Laplante and Nilson, 2011). One of the roles for these actomyosin cables could be to reorganize AJs during normal morphogenetic processes.

Characteristics of EPLIN-bearing AJs

EPLIN is known to bundle and stabilize actin fibers. This ability of EPLIN is likely a key process in maintaining ZAs. However, it inhibits Arp2/3-dependent branching of actin filaments (Maul et al., 2003), which suggests that EPLIN-bundled actin fibers are a rather static structure. This probably explains why the EPLIN-associated AJs look more static than EPLIN-free AJs.

We found that the αE-catenin–EPLIN fusion can form only lAJ-like contacts, which is consistent with the observation that native EPLIN participates in lAJ, but not pAJ, formation. The αE-catenin–EPLIN fusion-mediated junctions appeared unstable. Moreover, this artificial protein even disrupted the preformed junctions when introduced in DLD1 cells, probably by competing with the endogenous αE-catenin. Although it is unclear how much the artificial fusion proteins mimic the natural αE-catenin–EPLIN complex, some of the properties expressed by the fusion may reflect those of the natural complex. For example, the natural ZA may also be static, and not dynamic enough to engage in new contact formation; this could be a reason why cells need to convert the ZAs to pAJs at colony peripheries, so as to interact with other cells.

EPLIN and vinculin cooperate in AJ formation

The results obtained with the αE-catenin–EPLIN fusion proteins imply that, although the αE-catenin–EPLIN linkage is important for stabilizing the circumferential actin cables, its adhesion-sustaining ability may not be strong. We therefore thought that there must other proteins to support αE-catenin functions, and we reexamined the role of vinculin. αE-catenin mutants lacking the C-terminal EPLIN-binding region, such as αE(1–508), are able to organize AJs through the binding to vinculin (Watabe-Uchida et al., 1998; Yonemura et al., 2010). We showed that vinculin knockdown in αE(1–508)-R2/7 cells severely disrupted their junctions, which indicates that vinculin is essential for the adhesion-supporting ability of this construct. Normal DLD1 cells also responded to vinculin depletion, although these cells were not dissociated. In vinculin-depleted DLD1 cells, E-cadherin signals were no longer associated with pulling actin fibers, which suggested that vinculin plays a role in the E-cadherin–F-actin linkage, as observed in the integrin-mediated focal contacts (Geiger et al., 2009; Parsons et al., 2010). The reason why the junctions of DLD1 cells were more resistant to vinculin depletion than those of αE(1–508)-R2/7

cells can be explained by the previous observation that the C-terminal domain of αE-catenin, which is deleted in αE(1–508), has some ability to support αE-catenin–mediated cell adhesion, as assayed in fibroblastic cells (Imamura et al., 1999). Thus, αE-catenin seems to have multiple pathways for supporting cell–cell adhesion.

We previously proposed that EPLIN works as a linker between αE-catenin and F-actin. The present observations suggest that the αE-catenin–vinculin and αE-catenin–EPLIN complexes have distinct roles. It seems that the former is important for general AJ formation, and the latter is specified for ZA formation. To organize the complete set of AJs, they probably complement each other. It should be noted that αE(1–508) can organize both lAJs and pAJs, despite the absence of an EPLIN-binding site, which suggested that EPLIN need not be bound to αE-catenin for maintaining lAJs; that is, EPLIN could maintain ZA-associated actin filaments independently of the cadherin–catenin complex. However, the positioning of lAJs and pAJs in αE(1–508) transfectants is not well organized. This indicates that EPLIN assists the ordered ZA organization most efficiently through its binding to αE-catenin. For example, EPLIN senses tensed actomyosin fibers and recruits more cadherins to specific junctional sites via their linkages, strengthening the cell–cell adhesion there.

We have not determined whether vinculin and EPLIN bind together to a single αE-catenin or bind separately to different αE-catenin molecules when functioning at the ZAs. Notably, in αE(1–508)EPLIN-R2/7 cells, vinculin was concentrated at cell–cell junctions, probably through its binding to αE(1–508)EPLIN. This vinculin does not appear to be functional, however, as vinculin depletion did not affect these junctions. Thus, EPLIN and vinculin might compete with one another, even when they are linked to an αE-catenin molecule. In addition, we showed that αE(1–508) and αE(1–508)-EPLIN cotransfected into R2/7 cells organized a set of pAJ- and lAJ-like junctions, which suggests that EPLIN and vinculin can work through separate αE-catenin molecules. In conclusion, our findings suggest that EPLIN and vinculin cooperate in the proper organization of two forms of epithelial AJs, and that the mechanosensitive removal of the αE-catenin–EPLIN complex from AJs is involved in their morphological conversion, which is likely important for the reshaping of epithelial architecture at colony peripheries.

Materials and methods

Antibodies and reagents

For E-cadherin detection, rat monoclonal anti–E-cadherin (ECCD2; Shirayoshi et al., 1986) and mouse monoclonal anti–E-cadherin (HECD-1; Shimoyama et al., 1989) antibodies were used. Immunoglobulin fractions containing ECCD2 were purified from rat ascites fluids by 50% sodium ammonium sulfate fractionation and DEAE column chromatography. Antibodies against ROCK1 have been described previously (Nishimura and Takeichi, 2008). The following antibodies were purchased: rabbit polyclonal anti–αE-catenin, mouse monoclonal anti-vinculin, rabbit polyclonal anti-myosin IIA and IIB, and rabbit polyclonal anti–l-afadin antibodies (Sigma-Aldrich); rabbit polyclonal anti-myosin IIB antibody (Covance); rabbit polyclonal anti-EGFP antibody (MBL); mouse monoclonal anti-EPLIN antibody (BD); rabbit polyclonal anti–ZO-1 antibody (Invitrogen); and mouse monoclonal anti-glyceraldehyde 3-phosphate dehydrogenase (GAPDH; Millipore). F-actin was detected by Alexa Fluor 488– or Alexa Fluor 594–conjugated phalloidin (Invitrogen).

Plasmid construction

pCA-IRES-neomycin-mKOR and pCA-IRES-hygromycin-EGFP were used as the backbone plasmids for stable expression in eukaryotic cells, in which a neomycin- or hygromycin-resistant gene was driven by the IRES element. For construction of the full-length and mutant αE-catenins, 1–906 and 1–508 fragments were amplified from mouse αE-catenin cDNA (Kametani and Takeichi, 2007) by PCR, respectively. These DNA fragments were inserted into the EcoRV site of the backbone plasmids. Construction of EPLINβ-EGFP expression vectors was described previously (Abe and Takeichi, 2008). In brief, the full-length cDNA of mouse EPLIN, obtained from the Institute of Physical and Chemical Research FANTOM cDNA database, was amplified by PCR, and inserted into the NotI site of the backbone plasmid. For construction of αE(1–508)EPLIN, mouse EPLINβ cDNA (Abe and Takeichi, 2008) was amplified by PCR and inserted into the NotI site of pCA-IRES-hygromycin-αE(1–508)-EGFP, an enzyme site located in the 3′ side of the EcoRV site. Before this ligation, the NotI site was blunted with Blunting high (TOYOBO). These constructs were sequenced for conformation. Mouse E-cadherin was also cloned into the backbone vectors (constructed by Y. Kametani in our laboratory, RIKEN Center for Developmental Biology, Minatojima-Minamimachi, Chuo-ku, Kobe, Japan).

Cell culture and transfection

DLD1 and R2/7 (Watabe-Uchida et al., 1998) cells were cultured in a 1:1 mixture of DME and Ham's F12 medium (Iwaki) supplemented with 10% FCS, and maintained in 5% CO_2 at 37°C. Cells were transfected using Lipofectamine 2000 (Invitrogen) according to the manufacturer's instructions. For isolating stable transfectants, cells were selected by an exposure to 200 µg/ml of HygroGold (InvivoGen) and/or 400 µg/ml of G418. Mixtures of heterogeneous antibiotic-resistant clones were used for the analysis of transfectants to avoid clonal variations in the phenotypes. Y-27632 treatment was performed with the culture medium containing 20 µM of the reagent for 3 h in 5% CO_2 at 37°C. MCF10A cells were cultured with the MEGM Bullet kit (Takara Bio Inc.) containing 100 ng/ml cholera toxin (Sigma-Aldrich).

RNAi

Human EPLIN depletion was performed by using Stealth siRNAs (Invitrogen) whose sequence has been described previously (Abe and Takeichi, 2008). Transfection of EPLIN-specific siRNAs was performed with RNAiMAX (Invitrogen) according to the manufacturer's instructions: cells were treated with siRNA–RNAiMAX complexes for 4–5 h. Human vinculin depletion was performed using Mission siRNAs (Sigma-Aldrich). Sequences for the knockdown of vinculin were 5′-CAAGAUGAUUGACGAGAGATT-3′ or 5′-GAUUUACACUGCGCUGGGUTT-3′, designated as Nos. 3 and 7, respectively (Fig. 6 B). For the effective depletion of vinculin, the standard protocol was modified: cells were first treated with siRNA–RNAiMAX complexes for 3–5 h, and further cultured with fresh medium for 12–15 h. These cells were then trypsinized and replated on collagen-coated dishes (Iwaki) or coverslips (Iwaki) in the medium containing siRNA–RNAiMAX complexes. After 3–5 h, this medium was changed with fresh medium. After incubating for another 12–15 h, cells were subjected to analyses. When EPLIN and vinculin were co-depleted, the mixture of these siRNAs was used. Universal negative controls for each siRNA were obtained from Invitrogen and Sigma-Aldrich. For knockdown of myosin IIA and IIB, we used Mission siRNAs (Sigma-Aldrich) with the same protocol as used for vinculin depletion. Sequences for the knockdown of myosin IIA were 5′-GACAGAAUAGCUGAGUUCATT-3′ and 5′-GAGAUUGUGGAAAUGUACATT-3′, designated as Nos. 1 and 2, respectively (Fig. S5 A). For depletion of myosin IIB, sequences were 5′-GUCUGAUUUGCUUCUUGAATT-3′ and 5′-GCAGAAUUGACAUGCUUGATT-3′, designated as Nos. 2 and 3, respectively (Fig. S5 A). These siRNAs could deplete the expression of each isoform specifically.

Immunoprecipitation

Cells were washed with TMCN buffer (20 mM Tris-HCl, pH 7.4, 1 mM $MgCl_2$, 1 mM $CaCl_2$, and 0.15 M NaCl) containing 1 mM PMSF. These cells were harvested and dissolved in TMCN buffer containing 1% Nonidet P-40 and 1 mM PMSF on ice. This crude mixture was centrifuged at 200,000 *g* (for E-cadherin) or 17,400 *g* (for αE-catenin) for 30 min by Himac CS150NX (Hitachi) with an angle rotor (S110AT) at 4°C, and the supernatant was recovered. This supernatant was precleared with protein G–conjugated Sepharose beads (GE Healthcare) for 1 h. After removal of the Sepharose beads, the supernatant (lysate) was collected as the original fraction for immunoprecipitation. To obtain E-cadherin complexes from the lysate, immunoprecipitation was performed by using ECCD2 or anti–αE-catenin antibody. As a control, rat or rabbit normal

IgG (Beckman Coulter) was used. The complexes were precipitated with protein G–conjugated Sepharose beads, and eluted by SDS sample buffer (62.5 mM Tris-HCl, pH 6.8, 2% SDS, 0.003% Pyronin Y, and 10% glycerol) at 56°C for 15 min. Precipitates were separated by SDS-PAGE and analyzed by Western blotting. For detection of E-cadherin on the blots, HECD-1 antibody was used.

SDS-PAGE and Western blotting

Samples were denatured by heating with SDS sample buffer containing 1% 2-mercaptoethanol at 95°C for 3 min. Proteins were separated by SuperSep polyacrylamide gel (Wako Chemicals USA), and transferred to polyvinylidene difluoride membranes (Bio-Rad Laboratories). Membranes were blocked with 5% skim milk in TBS for 1 h at room temperature. Horseradish-conjugated secondary antibodies were purchased from GE Healthcare. Protein bands were detected by Western lightning plus ECL (PerkinElmer).

Immunostaining and confocal laser-scanning microscopy

Cells were fixed with 1% PFA in cultured medium for 10 min at room temperature. The fixed cells were permeabilized with 0.1% Triton X-100 in TBS, pH 7.4, for 10 min, and blocked with 5% skim milk in TBS for 10 min. Next, cells were incubated with primary antibodies in the blocking solution for 1–2 h. These cells were then washed with TBS and further treated with secondary antibodies. For double-staining, Alexa Fluor 488– or Alexa Fluor 594–conjugated antibodies (Invitrogen) were used as secondary antibodies. To detect ECCD2, CF Dye488A– or CF Dye594–conjugated antibodies (Biotium) were used. In the case of triple staining, ECCD2 was detected by Cy5-conjugated antibody (Millipore). These cells were washed with TBS and then with milliQ water (Millipore), and finally mounted with FluorSave (EMD). Images were acquired as a z stack (20–25 z sections, 0.3–0.5 µm apart, 1,024 × 1,024 pixels) through a Plan-Apochromat 63×/1.40 NA oil differential interference contrast microscopy objective lens (Carl Zeiss) with an inverted laser-scanning confocal microscope (LSM510; Carl Zeiss).

Live-cell imaging

Live-cell imaging was performed by using a Deltavision microscope (Applied Precision), unless otherwise specified. Before the operation, cells were cultured on collagen-coated glass-based dishes (Iwaki) with L-15 medium (Invitrogen) supplemented with 10% FCS for 1 h at 37°C. The dish was placed on the stage of an inverted microscope (IX70 or IX71; Olympus) equipped with a cooled charged-coupled device camera (Series 300 CH350 or CoolSNAP HQ2; Photometrics). The temperature of the microscope room was maintained at 37°C by a thermal controller (Sanyo). Time-lapse images (acquired as 6–10 z sections, 0.8–1.0 µm apart, 512 × 512 pixels, and binning 2 × 2) were obtained through Plan-Apochromat 60×/1.40 NA oil or Plan-Apochromat N60×/1.40 NA oil objective lenses.

Wound healing

Cells were cultured at confluent densities on collagen-coated coverslips (Iwaki) or glass-based dishes (Iwaki). Wound edges were generated by scraping cells with a plastic tip. After scraping, cells were cultured for another 3 h, fixed, and subjected to analyses. For live-cell imaging, cells were cultured with L-15 medium supplemented with 10% FCS for 30 min, scraped to generate wounds, and further cultured for 1 h. Time-lapse images were then collected for 4 h.

Laser ablation

Laser ablation was performed by using FluoView FV1000 laser-scanning confocal microscopy (Olympus) equipped with a laser ablation system (provided by T. Kondo and S. Hayashi, RIKEN Center for Developmental Biology, Kobe, Japan; UV-ASU-P2; Olympus). Under the monitor with confocal images, cells were irradiated with a laser beam (wavelength = 349 nm) at a specific spot. Time-lapse images (acquired as 4–8 z sections, 0.6–1.0 µm apart, and 512 × 512 pixels) were obtained with a UPLSAPO 60×/1.35 NA oil objective lens.

Image processing

For immunostaining, the digital images obtained by the LSM510 were processed using Photoshop 7.0 (Adobe). Projection of z-stack images were processed with LSM Image Browser (Carl Zeiss). For time-lapse imaging, digital images obtained by DeltaVision microscopy were processed and projected by using SoftWoRx (Applied Precision) and ImageJ. Sequential images were prepared from tiff-tagged files (8-bit grayscale or 24-bit RGB) using Photoshop 7.0. Digital images obtained by FV1000 microscopy were processed, and projected with FV10-ASW Ver. 2.0 Viewer and ImageJ. All videos were edited in the MOV format.

Application of mechanical stretch

Uniaxial mechanical stretch was applied to cell colonies by using a Strex system (ST-40; Strex; Iwaki et al., 2009), which was customized on DeltaVision microscope (Applied Precision). DLD1 cells were cultured on elastic chambers with L-15 medium (Invitrogen) supplemented with 10% FCS, and stretched to attain ∼150% of the original length, spending 24–30 s, and further maintained at the stretching state during image acquisition. After stretch of the elastic chamber, extension of the cells was confirmed by microscopic observation of E-cadherin–mKOR or EPLIN-EGFP signals. Images (acquired as 30 z sections, 1.0 µm apart, 512 × 512 pixels, and binning 2 × 2) were obtained through a LUCPlanFLN 60×/0.70 NA objective lens, and processed and analyzed with plot-profile by ImageJ. Scattergram was prepared with Excel (Microsoft). Signal intensity was quantified by ImageJ and analyzed by KaleidaGraph 4.0J.

Online supplemental material

Fig. S1 shows the distribution of AJ proteins in natural or scratched DLD1 colonies. Fig. S2 shows the distribution of various junctional proteins in DLD1 or MCF10A cells. Fig. S3 shows the distribution of exogenous EPLIN, and the ROCK dependence of EPLIN–AJ association. Fig. S4 shows the effects of laser ablation of peripheral actin fibers or ZA on E-cadherin distribution. Fig. S5 shows the effects of myosin II depletion on EPLIN localization in AJs. Video 1 shows time-lapse movies of E-cadherin–mKOR in DLD1 colonies. Video 2 shows a time-lapse movie of αE-catenin–EGFP during wound closure. Video 3 shows a time-lapse movie of actin-EGFP in DLD1 cells. Video 4 shows time-lapse movies of E-cadherin–mKOR in a confluent culture of control or EPLIN-depleted DLD1 cells. Video 5 shows a time-lapse movie of EPLIN-EGFP after ablation of peripheral actin fibers. Video 6 shows a time-lapse movie of EPLIN-EGFP and E-cadherin–mKOR after laser ablation of peripheral actin fibers. Video 7 shows a time-lapse movie of EPLIN-EGFP after ablation of a part of the ZA. Video 8 shows a time-lapse movie of αE(1–508)EPLIN-EGFP introduced into R2/7 cells. Video 9 shows a time-lapse movie of αE(1–508)-mKOR and αE(1–508)EPLIN-EGFP doubly introduced into R2/7 cells. Video 10 shows a time-lapse movie of αE(1–508)EPLIN-EGFP and E-cadherin–mKOR doubly introduced into DLD1 cells. Online supplemental material is available at http://www.jcb.org/cgi/content/full/jcb.201104124/DC1.

We thank Takefumi Kondo and Shigeo Hayashi for the laser ablation system; Shigenobu Yonemura, Shibata Tatsuo, and members of our laboratory for critical comments; and Toshihiko Ogura and Keiji Naruse for advice on cell-stretching methods.

This work was supported by a grant from Grants-in-Aid for Specially Promoted Research of the Ministry of Education, Science, Sports, and Culture of Japan (to M. Takeichi)

Submitted: 25 April 2011
Accepted: 18 July 2011

References

Abe, K., and M. Takeichi. 2008. EPLIN mediates linkage of the cadherin catenin complex to F-actin and stabilizes the circumferential actin belt. *Proc. Natl. Acad. Sci. USA*. 105:13–19. doi:10.1073/pnas.0710504105

Acloque, H., M.S. Adams, K. Fishwick, M. Bronner-Fraser, and M.A. Nieto. 2009. Epithelial-mesenchymal transitions: the importance of changing cell state in development and disease. *J. Clin. Invest.* 119:1438–1449. doi:10.1172/JCI38019

Adams, C.L., W.J. Nelson, and S.J. Smith. 1996. Quantitative analysis of cadherin-catenin-actin reorganization during development of cell-cell adhesion. *J. Cell Biol.* 135:1899–1911. doi:10.1083/jcb.135.6.1899

Boller, K., D. Vestweber, and R. Kemler. 1985. Cell-adhesion molecule uvomorulin is localized in the intermediate junctions of adult intestinal epithelial cells. *J. Cell Biol.* 100:327–332. doi:10.1083/jcb.100.1.327

Cavey, M., and T. Lecuit. 2009. Molecular bases of cell-cell junctions stability and dynamics. *Cold Spring Harb. Perspect. Biol.* 1:a002998. doi:10.1101/cshperspect.a002998

Drees, F., S. Pokutta, S. Yamada, W.J. Nelson, and W.I. Weis. 2005. Alpha-catenin is a molecular switch that binds E-cadherin-beta-catenin and regulates actin-filament assembly. *Cell*. 123:903–915. doi:10.1016/j.cell.2005.09.021

Farquhar, M.G., and G.E. Palade. 1963. Junctional complexes in various epithelia. *J. Cell Biol.* 17:375–412. doi:10.1083/jcb.17.2.375

Fernandez-Gonzalez, R., Sde.M. Simoes, J.C. Röper, S. Eaton, and J.A. Zallen. 2009. Myosin II dynamics are regulated by tension in intercalating cells. *Dev. Cell*. 17:736–743. doi:10.1016/j.devcel.2009.09.003

Franke, J.D., R.A. Montague, and D.P. Kiehart. 2005. Nonmuscle myosin II generates forces that transmit tension and drive contraction in multiple tissues during dorsal closure. *Curr. Biol.* 15:2208–2221. doi:10.1016/j.cub.2005.11.064

Geiger, B., K.T. Tokuyasu, A.H. Dutton, and S.J. Singer. 1980. Vinculin, an intracellular protein localized at specialized sites where microfilament bundles terminate at cell membranes. *Proc. Natl. Acad. Sci. USA*. 77:4127–4131. doi:10.1073/pnas.77.7.4127

Geiger, B., J.P. Spatz, and A.D. Bershadsky. 2009. Environmental sensing through focal adhesions. *Nat. Rev. Mol. Cell Biol.* 10:21–33. doi:10.1038/nrm2593

Gorfinkiel, N., and A.M. Arias. 2007. Requirements for adherens junction components in the interaction between epithelial tissues during dorsal closure in *Drosophila*. *J. Cell Sci.* 120:3289–3298. doi:10.1242/jcs.010850

Harris, T.J., J.K. Sawyer, and M. Peifer. 2009. How the cytoskeleton helps build the embryonic body plan: models of morphogenesis from *Drosophila*. *Curr. Top. Dev. Biol.* 89:55–85. doi:10.1016/S0070-2153(09)89003-0

Hildebrand, J.D. 2005. Shroom regulates epithelial cell shape via the apical positioning of an actomyosin network. *J. Cell Sci.* 118:5191–5203. doi:10.1242/jcs.02626

Imamura, Y., M. Itoh, Y. Maeno, S. Tsukita, and A. Nagafuchi. 1999. Functional domains of α-catenin required for the strong state of cadherin-based cell adhesion. *J. Cell Biol.* 144:1311–1322. doi:10.1083/jcb.144.6.1311

Ivanov, A.I., I.C. McCall, C.A. Parkos, and A. Nusrat. 2004. Role for actin filament turnover and a myosin II motor in cytoskeleton-driven disassembly of the epithelial apical junctional complex. *Mol. Biol. Cell*. 15:2639–2651. doi:10.1091/mbc.E04-02-0163

Ivanov, A.I., M. Bachar, B.A. Babbin, R.S. Adelstein, A. Nusrat, and C.A. Parkos. 2007. A unique role for nonmuscle myosin heavy chain IIA in regulation of epithelial apical junctions. *PLoS ONE*. 2:e658. doi:10.1371/journal.pone.0000658

Iwaki, M., S. Ito, M. Morioka, S. Iwata, Y. Numaguchi, M. Ishii, M. Kondo, H. Kume, K. Naruse, M. Sokabe, and Y. Hasegawa. 2009. Mechanical stretch enhances IL-8 production in pulmonary microvascular endothelial cells. *Biochem. Biophys. Res. Commun.* 389:531–536. doi:10.1016/j.bbrc.2009.09.020

Jacinto, A., W. Wood, T. Balayo, M. Turmaine, A. Martinez-Arias, and P. Martin. 2000. Dynamic actin-based epithelial adhesion and cell matching during *Drosophila* dorsal closure. *Curr. Biol.* 10:1420–1426. doi:10.1016/S0960-9822(00)00796-X

Kalluri, R., and R.A. Weinberg. 2009. The basics of epithelial-mesenchymal transition. *J. Clin. Invest.* 119:1420–1428. doi:10.1172/JCI39104

Kametani, Y., and M. Takeichi. 2007. Basal-to-apical cadherin flow at cell junctions. *Nat. Cell Biol.* 9:92–98. doi:10.1038/ncb1520

Kovacs, E.M., and A.S. Yap. 2008. Cell-cell contact: cooperating clusters of actin and cadherin. *Curr. Biol.* 18:R667–R669. doi:10.1016/j.cub.2008.06.024

Kwiatkowski, A.V., S.L. Maiden, S. Pokutta, H.J. Choi, J.M. Benjamin, A.M. Lynch, W.J. Nelson, W.I. Weis, and J. Hardin. 2010. In vitro and in vivo reconstitution of the cadherin-catenin-actin complex from Caenorhabditis elegans. *Proc. Natl. Acad. Sci. USA*. 107:14591–14596. doi:10.1073/pnas.1007349107

Ladoux, B., E. Anon, M. Lambert, A. Rabodzey, P. Hersen, A. Buguin, P. Silberzan, and R.M. Mège. 2010. Strength dependence of cadherin-mediated adhesions. *Biophys. J.* 98:534–542. doi:10.1016/j.bpj.2009.10.044

Laplante, C., and L.A. Nilson. 2011. Asymmetric distribution of Echinoid defines the epidermal leading edge during *Drosophila* dorsal closure. *J. Cell Biol.* 192:335–348. doi:10.1083/jcb.201009022

Lecuit, T. 2005. Adhesion remodeling underlying tissue morphogenesis. *Trends Cell Biol.* 15:34–42. doi:10.1016/j.tcb.2004.11.007

le Duc, Q., Q. Shi, I. Blonk, A. Sonnenberg, N. Wang, D. Leckband, and J. de Rooij. 2010. Vinculin potentiates E-cadherin mechanosensing and is recruited to actin-anchored sites within adherens junctions in a myosin II-dependent manner. *J. Cell Biol.* 189:1107–1115. doi:10.1083/jcb.201001149

Maul, R.S., Y. Song, K.J. Amann, S.C. Gerbin, T.D. Pollard, and D.D. Chang. 2003. EPLIN regulates actin dynamics by cross-linking and stabilizing filaments. *J. Cell Biol.* 160:399–407. doi:10.1083/jcb.200212057

Meng, W., and M. Takeichi. 2009. Adherens junction: molecular architecture and regulation. *Cold Spring Harb. Perspect. Biol.* 1:a002899. doi:10.1101/cshperspect.a002899

Miyake, Y., N. Inoue, K. Nishimura, N. Kinoshita, H. Hosoya, and S. Yonemura. 2006. Actomyosin tension is required for correct recruitment of adherens junction components and zonula occludens formation. *Exp. Cell Res.* 312:1637–1650. doi:10.1016/j.yexcr.2006.01.031

Montell, D.J. 2008. Morphogenetic cell movements: diversity from modular mechanical properties. *Science*. 322:1502–1505. doi:10.1126/science.1164073

Nelson, W.J. 2008. Regulation of cell-cell adhesion by the cadherin-catenin complex. *Biochem. Soc. Trans.* 36:149–155. doi:10.1042/BST0360149

Nishimura, T., and M. Takeichi. 2008. Shroom3-mediated recruitment of Rho kinases to the apical cell junctions regulates epithelial and neuroepithelial planar remodeling. *Development*. 135:1493–1502. doi:10.1242/dev.019646

Parsons, J.T., A.R. Horwitz, and M.A. Schwartz. 2010. Cell adhesion: integrating cytoskeletal dynamics and cellular tension. *Nat. Rev. Mol. Cell Biol.* 11:633–643. doi:10.1038/nrm2957

Perez-Moreno, M., C. Jamora, and E. Fuchs. 2003. Sticky business: orchestrating cellular signals at adherens junctions. *Cell*. 112:535–548. doi:10.1016/S0092-8674(03)00108-9

Sawyer, J.K., N.J. Harris, K.C. Slep, U. Gaul, and M. Peifer. 2009. The *Drosophila* afadin homologue Canoe regulates linkage of the actin cytoskeleton to adherens junctions during apical constriction. *J. Cell Biol.* 186:57–73. doi:10.1083/jcb.200904001

Schwartz, M.A., and D.W. DeSimone. 2008. Cell adhesion receptors in mechanotransduction. *Curr. Opin. Cell Biol.* 20:551–556. doi:10.1016/j.ceb.2008.05.005

Shimoyama, Y., S. Hirohashi, S. Hirano, M. Noguchi, Y. Shimosato, M. Takeichi, and O. Abe. 1989. Cadherin cell-adhesion molecules in human epithelial tissues and carcinomas. *Cancer Res.* 49:2128–2133.

Shirayoshi, Y., A. Nose, K. Iwasaki, and M. Takeichi. 1986. N-linked oligosaccharides are not involved in the function of a cell-cell binding glycoprotein E-cadherin. *Cell Struct. Funct.* 11:245–252. doi:10.1247/csf.11.245

Small, J.V., and G.P. Resch. 2005. The comings and goings of actin: coupling protrusion and retraction in cell motility. *Curr. Opin. Cell Biol.* 17:517–523. doi:10.1016/j.ceb.2005.08.004

Smutny, M., H.L. Cox, J.M. Leerberg, E.M. Kovacs, M.A. Conti, C. Ferguson, N.A. Hamilton, R.G. Parton, R.S. Adelstein, and A.S. Yap. 2010. Myosin II isoforms identify distinct functional modules that support integrity of the epithelial zonula adherens. *Nat. Cell Biol.* 12:696–702. doi:10.1038/ncb2072

Solon, J., A. Kaya-Copur, J. Colombelli, and D. Brunner. 2009. Pulsed forces timed by a ratchet-like mechanism drive directed tissue movement during dorsal closure. *Cell*. 137:1331–1342. doi:10.1016/j.cell.2009.03.050

Tamada, M., T.D. Perez, W.J. Nelson, and M.P. Sheetz. 2007. Two distinct modes of myosin assembly and dynamics during epithelial wound closure. *J. Cell Biol.* 176:27–33. doi:10.1083/jcb.200609116

Thiery, J.P. 2002. Epithelial-mesenchymal transitions in tumour progression. *Nat. Rev. Cancer*. 2:442–454. doi:10.1038/nrc822

Vasioukhin, V., and E. Fuchs. 2001. Actin dynamics and cell-cell adhesion in epithelia. *Curr. Opin. Cell Biol.* 13:76–84. doi:10.1016/S0955-0674(00)00177-0

Vasioukhin, V., C. Bauer, M. Yin, and E. Fuchs. 2000. Directed actin polymerization is the driving force for epithelial cell-cell adhesion. *Cell*. 100:209–219. doi:10.1016/S0092-8674(00)81559-7

Watabe-Uchida, M., N. Uchida, Y. Imamura, A. Nagafuchi, K. Fujimoto, T. Uemura, S. Vermeulen, F. van Roy, E.D. Adamson, and M. Takeichi. 1998. α-Catenin-vinculin interaction functions to organize the apical junctional complex in epithelial cells. *J. Cell Biol.* 142:847–857. doi:10.1083/jcb.142.3.847

Welch, M.D., A. Mallavarapu, J. Rosenblatt, and T.J. Mitchison. 1997. Actin dynamics in vivo. *Curr. Opin. Cell Biol.* 9:54–61. doi:10.1016/S0955-0674(97)80152-4

Yamada, S., S. Pokutta, F. Drees, W.I. Weis, and W.J. Nelson. 2005. Deconstructing the cadherin-catenin-actin complex. *Cell*. 123:889–901. doi:10.1016/j.cell.2005.09.020

Yonemura, S., M. Itoh, A. Nagafuchi, and S. Tsukita. 1995. Cell-to-cell adherens junction formation and actin filament organization: similarities and differences between non-polarized fibroblasts and polarized epithelial cells. *J. Cell Sci.* 108:127–142.

Yonemura, S., Y. Wada, T. Watanabe, A. Nagafuchi, and M. Shibata. 2010. alpha-Catenin as a tension transducer that induces adherens junction development. *Nat. Cell Biol.* 12:533–542. doi:10.1038/ncb2055

Ziegler, W.H., R.C. Liddington, and D.R. Critchley. 2006. The structure and regulation of vinculin. *Trends Cell Biol.* 16:453–460. doi:10.1016/j.tcb.2006.07.004